Cell Biology International

Cell Biol. Int. (2010) 34, 433–439 (Printed in Great Britain)

Research Article

Regulatory role of the extreme C-terminal end of the S6 inner helix in C-terminal-truncated Kv1.2 channel activation

Li-Li Zhao*,†, Zhi Qi‡, Xian-En Zhang§, Li-Jun Bi[1]* and Gang Jin[1]*

* National Laboratory of Biomacromolecules, Institute of Biophysics, Chinese Academy of Sciences, 15 Datun Rd, Beijing 100101, China
† National Institute for Communicable Disease Control and Prevention, Chinese Center for Disease Control and Prevention/State Key Laboratory for Infectious Disease Prevention and Control, Beijing 102206, China
‡ State Key Laboratory of Brain and Cognitive Science, Institute of Biophysics, Chinese Academy of Sciences, 15 Datun Rd, Beijing 100101, China
§ State Key Laboratory of Virology, Wuhan Institute of Virology, Chinese Academy of Sciences, Wuhan 430071, China

Abstract

The transmembrane part of the S6 inner helix of the Kv1.2 potassium channel is a pivotal part in sustaining channel activity. However, the role of its extreme C-terminal end, which is located on the cytoplasmic side of the channel, is largely unknown. Here, we investigated the role of the extreme C-terminal end of the S6 inner helix (the HRET region) by constructing a series of C-terminal-truncated mutations related to this region in the C-terminal-truncated Kv1.2 channel. Mutations on Thr^{421} or Glu^{420} significantly altered the activation of the truncated channel. Mutations on Arg^{419} demonstrated that neutral or basic, but not acidic amino acid, is essential at the position for the truncated channel activation, and no functional channel was observed when the channel was truncated from His^{418}. Hence, our results indicate that the extreme C-terminal end of the S6 inner helix plays an important regulatory role in the activation of the C-terminal-truncated Kv1.2 channel.

Keywords: activation; Kv1.2 channel; patch-clamp; surface expression; S6 inner helix

1. Introduction

The Kv1.2 channel is a low-threshold, rapidly activating voltage-gated potassium channel in mammalian neurons (Stuhmer et al., 1989). It plays fundamental roles in generating electrical pulses and regulating membrane potential in brain and neuronal connections (Hoshi et al., 1990). The physiological importance of the Kv1.2 channel has been underscored by the recent findings that the Kv1.2 knockout mice exhibit enhanced seizure susceptibility and die in the third postnatal week (Brew et al., 2007).

The mature Kv1.2 potassium channels are tetramers, with each subunit containing six transmembrane segments that are named S1-S6. The S1-S4 segments form the region that senses changes in membrane voltage. The S5-S6 segments form the ion conduction pore, providing a pathway for ions to cross the membrane in the open state. When the channel closes, ion permeation is minimized by an activation gate that locates near the intracellular entrance to the pore in the S6 segment (Holmgren et al., 1997, 1998; del Camino and Yellen, 2001; Zhou et al., 2001; Hackos et al., 2002; Soler-Llavina et al., 2006). The recently solved crystal structure of the Kv1.2 channel reveals that the C-terminus (PVPVIVSNFNYFY) of the S6 inner helix forms a platform for the S4-S5 linker, so that they can correctly interact with each other (Long et al., 2005a). It has been proposed that the motions of the S4 helices are transmitted to the S6 inner helix of the channel, via the S4-S5 linker, to promote the channel opening or closing (Long et al., 2005a). Hence, the S6 inner helix is presumed to be necessary for the functional voltage-dependent Kv1.2 channel. This has been proved by a series of mutation experiments. For example, mutations in the Pro–X–Pro sequence of the S6 inner helix of Kv channels have profound effects on gating (Liu et al., 1997; Schoppa and Sigworth, 1998; Hackos et al., 2002; Yifrach and MacKinnon, 2002; Soler-Llavina et al., 2006). Moreover, mutants that lack the preceding NFN, YFY or other combinations of residues in the S6 inner helix do not express current (Lu et al., 2001, 2002).

As for the HRET region located immediately downstream from the PVPVIVSNFNFNYFY (Figure 1), it is only known that a truncation in this region in the Kv1.1 channel is related to human EA-1 (episodic ataxia type-1) (Eunson et al., 2000). Because the HRET region is highly conserved in Kv1 channels, we supposed that the HRET region probably played important roles for the Kv1.2 channel.

Here we addressed the function of the HRET region in the Kv1.2 channel by constructing a series of C-terminal truncations related to the region. In Shaker family Kv channels, the cytoplasmic C-termini are involved in many processes that range from channel gating (Hopkins et al., 1994; Jerng and Covarrubias, 1997) to voltage sensitivity (Marten and Hoshi, 1998). Therefore, to

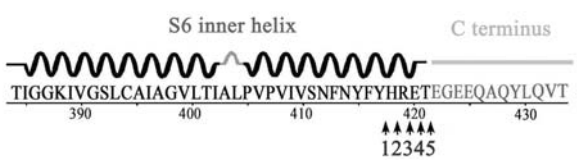

Figure 1 The S6 inner helix and part of the C terminus sequence of the Kv1.2 potassium channel (NP_037102)

Arrow heads indicate the five truncating sites. 1: $Kv1.2_{417stop}$, 2: $Kv1.2_{418stop}$, 3: $Kv1.2_{419stop}$, 4: $Kv1.2_{420stop}$, 5: $Kv1.2_{421stop}$.

[1] Correspondence may be addressed to either of these authors (email blj@sun5.ibp.ac.cn or gajin@imech.ac.cn).

Abbreviations: CHO, Chinese hamster ovary; EGFP, enhanced green fluorescent protein; $EGFP^+PE^+$, EGFP and PE positive; *G*, conductance; *I*, current amplitude; PE, phycoerythrin; *V*, test potential.

avoid the influence of the cytoplasmic C-terminus, we removed the whole C-terminus of the channel in our experiments. Our observation demonstrated that this region not only plays important roles in regulating the activation of the C-terminal-truncated Kv1.2 channel, but also affects the expression level of the truncated channel on the plasma membrane.

2. Materials and methods

2.1. DNA constructs and mutagenesis

Rat brain Kv1.2 cDNA was a gift of Dr YN Jan (Departments of Physiology and Biochemistry, Howard Hughes Medical Institute, University of California, San Francisco, U.S.A.). All DNA sequences of mutants were obtained through PCR-based mutagenesis and subcloned into pcDNA3.1(−) vectors (Invitrogen) between BamHI and HindIII sites for expression in mammalian cells. The sequences of the inserted segments were confirmed by the DNA sequencing.

2.2. Expression of the channels in CHO (Chinese hamster ovary) cells

CHO–K1 cells were maintained in continuous culture. The cells were transiently co-transfected with recombination plasmids and pEGFP (Clontech) plasmids at a ratio of 5:1 (weight/weight) using LipofectAMINE Plus^{TM} reagent (Invitrogen) and assayed for electrophysiological measurements 24–48 h after transfection.

2.3. Electrophysiological recordings

Voltage-clamp recordings were performed using the EPC-9 patch-clamp amplifier (HEKA). Pipette and membrane capacitances were compensated automatically with the amplifier. Pipette-to-bath resistances ranged between 2 and 4 MΩ with intracellular solution containing (in mM): 140 KCl, 2 $MgCl_2$, 2 $CaCl_2$, 1 EGTA, 2 Na_2ATP and 10 HEPES at pH 7.3 (KOH). The bath solution was HBSS (Hanks' balanced salts solution, Sigma) containing (in mM): 1.3 $CaCl_2$, 0.8 $MgSO_4$, 5.4 KCl, 0.4 KH_2PO_4, 136.9 NaCl, 0.3 Na_2PO_4, 10 D-glucose and 4.2 $NaHCO_3$. The membrane potential was held at −100 mV and depolarized for 300 ms to +80 mV in 20 mV increments. Non-transfected CHO cells exhibited no voltage-gated or very small whole cell outward currents (50–100 pA), whereas cells transfected with wild-type Kv1.2 channels and some Kv1.2 mutations exhibited currents greater than 1nA. All results were repeated three times with ⩾3 cells in each experiment. All experiments were performed at room temperature (23–25°C).

2.4. FACS analysis

Kv1.2, Kv1.2$_{419stop}$ and Kv1.2$_{418stop}$ were engineered with the flag epitope (DYKDDDDK) on D^{194} of their extracellular S1–S2 linkers. EGFP-Kv1.2-flag, EGFP-Kv1.2$_{419stop}$-flag and EGFP-Kv1.2$_{418stop}$-flag were constructed by inserting the coding sequence of EGFP (enhanced green fluorescent protein; Clontech) into these three reconstructed vectors between NheI and BamHI sites. All these sequences were confirmed by DNA sequencing. The three reconstructed plasmids were transfected into CHO cells respectively. After 24–36 h, the transfected CHO cells were washed three times with PBS and incubated with PE (phycoerythrin)-labelled mouse anti-flag antibody (Martek Biosciences) for 30 min at 37°C. The transfected cells without the antibody served as the blank control. After being washed three times, the cells were then resuspended in PBS for quantifying the fluorescence by flow cytometry as described (Nesti et al., 2004). WinMDI 2.9 software (J. Trotter, Scripps Research Institute, La Jolla, CA) was used for flow cytometry data analysis. EGFP positive (EGFP$^+$) cells denoted the cells expressing the Kv1.2 channel or its truncations. EGFP and EGFP$^+$PE$^+$ (EGFP and PE positive) cells denoted the cells with surface expression of the Kv1.2 channel or its truncations. Relative surface expression level was calculated as the number of EGFP$^+$PE$^+$ cells divided by that of EGFP$^+$ cells. The relative surface expression level of EGFP-Kv1.2-flag was set at 1.0.

2.5. Data analysis

Data were analysed with Origin 7.0 (Origin Lab). The peak I (current amplitude) at each test potential was converted into G (conductance) using the equation

$$G=I/(V-E_K)$$

The Nernst potassium ion equilibrium potential E_k was calculated as −84 mV. The normalized conductance G was plotted against the V (test potential) and fitted to a single Boltzmann equation

$$G/G_{max}=1/\{1+\exp[-(V-V_{1/2})/k]\}$$

where G_{max} is the maximum conductance, $V_{1/2}$ is the voltage at half-maximal activation and k is the slope factor. The activation time constant was fitted with one exponential component according to

$$I=A^*[1-\exp(-t/\tau)]$$

Data are expressed as mean ± S.E.M. Significance among multiple groups was determined by ANOVA (one-way analysis of variance). Statistical significance was set at $P<0.05$.

3. Results

3.1. Functional Kv1.2 channel without cytoplasmic C-terminus

To investigate the effect of the extreme C-terminal end of the S6 inner helix in the Kv1.2 potassium channel activation, we truncated the C-terminus at Thr^{421} site to obtain the Kv1.2$_{421stop}$ truncated channel, in which the cytoplasmic C-terminus of the

channel was completely deleted. This truncation and the wild-type Kv1.2 channel were each co-transfected into CHO cells with EGFP to facilitate detection of the transfected cells. Fluorescent cells were selected for electrophysiological measurement. Cells transfected with the wild-type and the truncated Kv1.2 channel ($Kv1.2_{421stop}$) are both functional (Figure 2A). This result indicates that the cytoplasmic C-terminus is not essential for forming a functional Kv1.2 channel.

The activation properties of Kv1.2 channels are highly variable, with reported $V_{1/2}$ values ranging from −40 to +30 mV (Grissmer et al., 1994; Steidl and Yool, 1999; Minor et al., 2000; Scholle et al., 2004; Rezazadeh et al., 2007). Here our results showed the $V_{1/2}$ value was 17.5 ± 1.9 mV for the Kv1.2 channel (n=9). Compared to the wild type, the $Kv1.2_{421stop}$ truncated channel ($V_{1/2}$: −1.8 ± 2.9 mV, n=8) caused the activation curve of the channel to shift by ≈20 mV towards hyperpolarizing potentials (Figures 2B and 2C). Furthermore, the activation time constant was also significantly altered with the mutation. The activation constant was 7.2 ± 1.4 ms for the wild-type Kv1.2 channel, while it was 3.0 ± 0.7 ms for the $Kv1.2_{421stop}$ truncated channel at +40 mV (Figure 2D). These differences suggested that the cytoplasmic C-terminus of the Kv1.2 channel could affect the activity of the channel.

3.2. Regulatory role of Thr^{421} in the activation of the channel

To understand the role of Thr^{421} on the channel activation, we introduced mutations of T421A ($Kv1.2_{T421Astop}$) and T421S ($Kv1.2_{T421Sstop}$) on the $Kv1.2_{421stop}$ channel. Analysis of the activation curves revealed that the $V_{1/2}$ value was 28.3 ± 2.5 mV for the $Kv1.2_{T421Astop}$ (n=8) or 24.2 ± 3.0 mV for the $Kv1.2_{T421Sstop}$ (n=7) (Figures 2B and C), shifted by ⩾26 mV towards depolarizing potentials compared to that of the $Kv1.2_{421stop}$ channel. Similarly, the activation time constants for both the $Kv1.2_{T421Astop}$ (8.3 ± 1.4 ms) and the $Kv1.2_{T421Sstop}$ (8.1 ± 2.0 ms) were significantly different from that of the $Kv1.2_{421stop}$ channel (3.0 ± 0.7 ms) at +40 mV (Figure 2D).

We continued to delete the Thr^{421} on the $Kv1.2_{421stop}$ channel to obtain $Kv1.2_{420stop}$ truncation. In contrast with $Kv1.2_{421stop}$ truncation, the activation curve of the $Kv1.2_{420stop}$ truncated

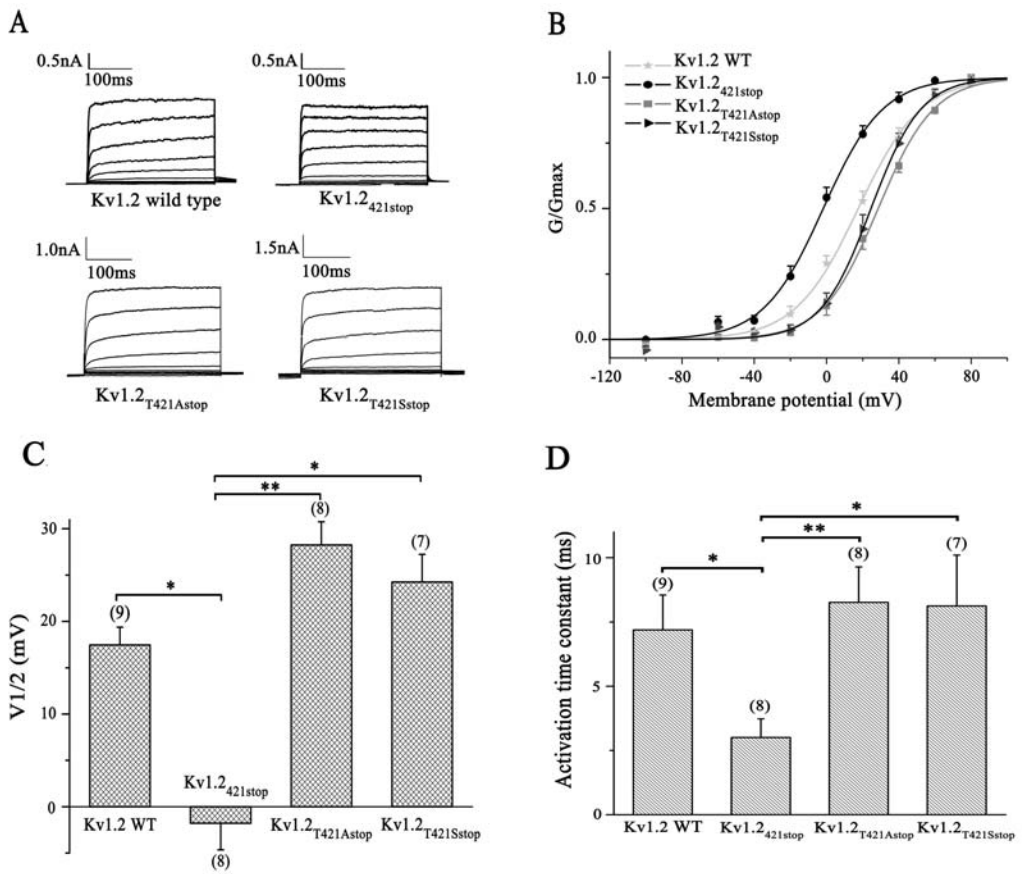

Figure 2 The roles of Thr^{421} on the activation of the Kv1.2 truncated channel

(**A**) Current records from Kv1.2 wild type, $Kv1.2_{421stop}$, $Kv1.2_{T421Astop}$ and $Kv1.2_{T420Sstop}$. Holding potential was −100 mV, and depolarizations were from −100 to 80 mV, in 20 mV increments. (**B**) Activation curves of Kv1.2 wild type, $Kv1.2_{421stop}$, $Kv1.2_{T421Astop}$ and $Kv1.2_{T420Sstop}$ channels. Smooth curves through the data represent fits to the mean values with the Boltzmann function. (**C**) Statistics on $V_{1/2}$ values of Kv1.2 wild type, $Kv1.2_{421stop}$, $Kv1.2_{T421Astop}$ and $Kv1.2_{T421Sstop}$ channels. (**D**) Statistics on the activation time constants of Kv1.2 wild type, $Kv1.2_{421stop}$, $Kv1.2_{T421Astop}$ and $Kv1.2_{T421Sstop}$ channels at +40 mV. Numbers in parentheses represent the total number of independent experiments. Significant difference was analysed by comparing $Kv1.2_{421stop}$ with Kv1.2 channel, and $Kv1.2_{421stop}$ with each of its mutants. *P<0.05. **P<0.01.

channel shifted significantly to more positive potentials ($V_{1/2}$: 22.5±1.3 mV, n=5) (P<0.0001), which is similar to those of the Kv1.2$_{421stop}$ mutations (Kv1.2$_{T421Astop}$ and Kv1.2$_{T421Sstop}$). The activation time constant of Kv1.2$_{420stop}$ (6.3±1.5 ms) at +40 mV was also different from that of Kv1.2$_{421stop}$ and similar to those of the Kv1.2$_{421stop}$ mutations (Kv1.2$_{T421Astop}$ and Kv1.2$_{T421Sstop}$). Hence, mutating or deleting the last amino acid of the S6 inner helix (Thr^{421}) shifted the activation curve with significant difference in the $V_{1/2}$ values.

3.3. Regulatory role of Glu^{420} in the activation of the channel

Next, we examined the function of Glu^{420}, which is the only amino acid carrying a hydrophilic acidic group with strong negative charge in the HRET region. At first, Glu^{420} was mutated to acidic amino acid, aspartic acid (Kv1.2$_{E420Dstop}$); neutral amino acid, alanine (Kv1.2$_{E420Astop}$); or basic amino acid, arginine (Kv1.2$_{E420Rstop}$) respectively. The G–V curve for the Kv1.2$_{E420Dstop}$ ($V_{1/2}$: 28.7±2.5 mV, n=6) shifted slightly towards depolarizing potentials compared with the Kv1.2$_{420stop}$ channel (Figures 3A and 3B). In contrast with the acidic acid substitution at Glu^{420}, mutations to alanine ($V_{1/2}$: 10.9±2.5 mV, n=5) and arginine ($V_{1/2}$: 11.8±3.8 mV, n=6) caused large negative shifts in the activation G–V curves. The activation time constants of Kv1.2$_{420stop}$ mutations at +40 mV are 5.6±1.6 ms for Kv1.2$_{E420Dstop}$, 4.2±1.6 ms for Kv1.2$_{E420Astop}$ and 4.5±0.8 ms for Kv1.2$_{E420Rstop}$ (Figure 3C).

Then, we truncated Glu^{420} on the Kv1.2$_{420stop}$ channel to produce the Kv1.2$_{419stop}$ truncation. For the G–V relationship, Kv1.2$_{419stop}$ ($V_{1/2}$: 5.9±3.9 mV, n=6) was very similar to Kv1.2$_{E420Astop}$, but shifted significantly to the left compared with Kv1.2$_{420stop}$ (P<0.01), Kv1.2$_{E420Dstop}$ and Kv1.2$_{E420Rstop}$. These findings demonstrated that the negative charge at the position of 420 is critical to the voltage-dependent gating of the channel.

3.4. Regulatory role of Arg^{419} in the activation of the channel

To get insight into the effects of Arg^{419}, we mutated it to positively charged lysine (Kv1.2$_{R419Kstop}$), hydrophobic leucine (Kv1.2$_{R419Lstop}$), hydrophilic asparagine (Kv1.2$_{R419Nstop}$) and negatively charged aspartic acid (Kv1.2$_{R419Dstop}$) respectively. The activation curve of the mutated channel was similar to that of Kv1.2$_{419stop}$ when the arginine was replaced by lysine (Kv1.2$_{R419Kstop}$: $V_{1/2}$=6.5±2.7 mV, n=6) or hydrophobic leucine (Kv1.2$_{R419Lstop}$: $V_{1/2}$=10.3±3.5 mV, n=7), but shifted largely to more positive potentials with the arginine substituted by a hydrophilic neutral amino acid (Kv1.2$_{R419Nstop}$: $V_{1/2}$=16.5±2.5 mV, n=6) (Figures 4A and 4B). Figure 4C showed the activation time constant of Kv1.2$_{419stop}$ and mutated channels at +40 mV. The τ values of these channels were 4.9±1.4 ms for Kv1.2$_{419stop}$, 3.8±0.8 ms for Kv1.2$_{R419Kstop}$, 4.9±0.9 ms for Kv1.2$_{R419Lstop}$ and 6.7±2.0 ms for Kv1.2$_{R419Nstop}$ respectively. Thus, the hydrophobic property of the amino acid at the site 419 has influence on

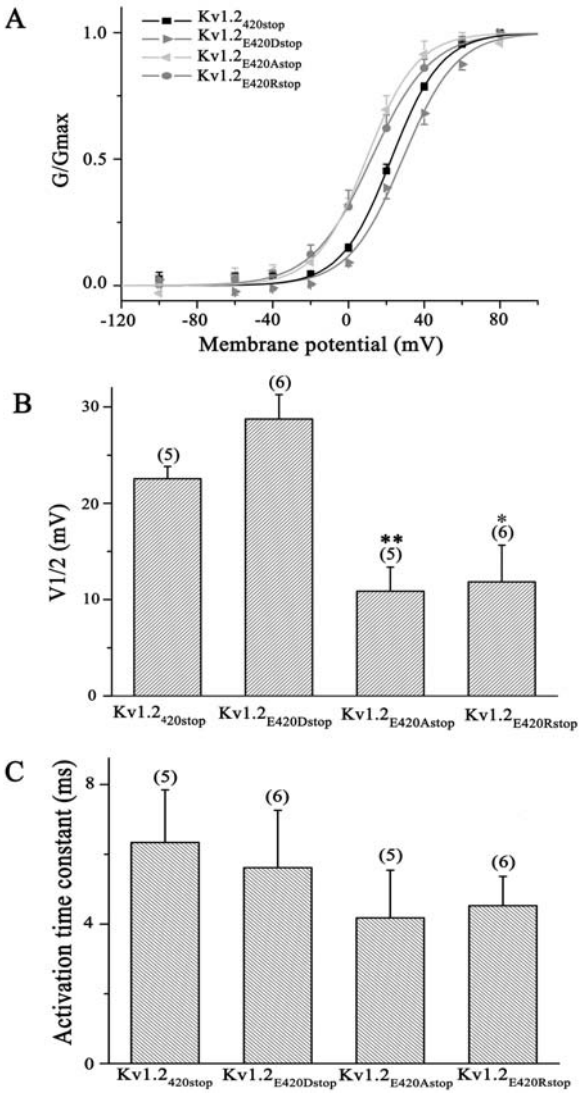

Figure 3 Effects of Glu^{420} on the activation of the Kv1.2 truncated channel
(**A**) Activation curves for the Kv1.2$_{420stop}$, Kv1.2$_{E420Dstop}$, Kv1.2$_{E420Astop}$ and Kv1.2$_{E420Rstop}$ channels. (**B**) Statistics on the $V_{1/2}$ values of the Kv1.2$_{420stop}$ and mutated channels. (**C**) The activation time constants of the Kv1.2$_{420stop}$ and mutated channels at +40 mV.

the activation of the channel. However, there was no functional channel current when the positively charged Arg^{419} was mutated to negatively charged aspartic acid (n=14). This result meant that a non-negatively charged amino acid at 419 is necessary for the channel function.

We further truncated Arg^{419} to produce the Kv1.2$_{418stop}$ truncation, which added the stop codon after residue His^{418} to the C-terminal end. After deletion of the whole C-terminus of the Kv1.2 channel and the last two residues of the S6 inner helix, Kv1.2$_{419stop}$ could express voltage-activated outward currents. However, deletion of more amino acid residues of the S6 inner helix, i.e. Kv1.2$_{418stop}$ and Kv1.2$_{417stop}$, no longer produced functional channels despite increase in the amount of the plasmids (n=19 for Kv1.2$_{418stop}$ and n=13 for Kv1.2$_{417stop}$). This finding suggested that Arg^{419} was critical in sustaining channel function.

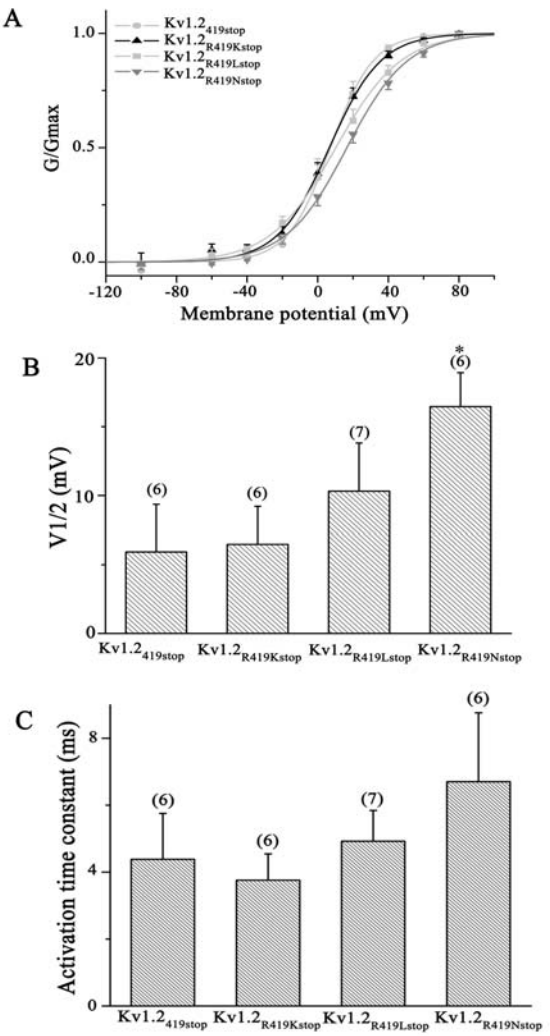

Figure 4 Effects of Arg^{419} substitutions on the activation of the truncated channel

(**A**) Activation curves for the mutated Kv1.2$_{419stop}$ channels, in which the Arg^{419} was mutated to lysine (Kv1.2$_{R419Kstop}$), leucine (Kv1.2$_{R419Lstop}$) and asparagine (Kv1.2$_{R419Nstop}$) respectively. (**B**) Statistics on the $V_{1/2}$ values of the wild-type and the mutated Kv1.2$_{419stop}$ channels. (**C**) The activation time constants of the Kv1.2$_{419stop}$ and mutated channels at +40 mV.

3.5. Membrane surface expression of Kv1.2$_{419stop}$ and Kv1.2$_{418stop}$

To judge if the non-functional Kv1.2$_{418stop}$ channel is a result of its inability to express on the membrane, we used flow cytometry to detect the fluorescent anti-flag antibody bound to the EGFP-Kv1.2$_{418stop}$-flag, EGFP-Kv1.2$_{419stop}$-flag and EGFP-Kv1.2-flag. The EGFP-Kv1.2$_{418stop}$-flag truncation exhibited fewer EGFP$^+$PE$^+$ cells compared with that of the EGFP-Kv1.2$_{419stop}$-flag channel and the EGFP-Kv1.2-flag channel (Figure 5A). The surface expression level of the channels was obtained by dividing the number of EGFP$^+$PE$^+$ cells by the number of EGFP$^+$ cells. Normalized to the surface expression level of the Kv1.2 channel, the relative surface expression level was 22% and 56% for the

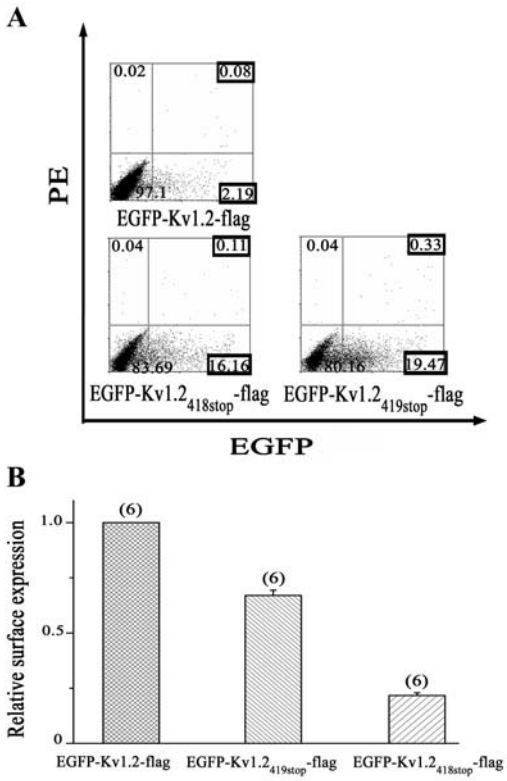

Figure 5 Cell surface expression of Kv1.2$_{419stop}$ and Kv1.2$_{418stop}$ channels

(**A**) The percentage of EGFP$^+$PE$^+$ cells and EGFP$^+$ cells (both highlighted in black box) among transfected EGFP-Kv1.2, EGFP-Kv1.2-flag, EGFP-Kv1.2$_{419stop}$-flag and EGFP-Kv1.2$_{418stop}$-flag CHO cells respectively. (**B**) Relative surface expression levels calculated by dividing cells with channel expressed on membrane surface (EGFP$^+$PE$^+$ cells) by cells with channel (EGFP$^+$ cells). Times of each independent experiment are indicated in parentheses.

Kv1.2$_{418stop}$ and Kv1.2$_{419stop}$ channels respectively (Figure 5B). Though the Kv1.2$_{418stop}$ channel had a lower expression on cell membrane than Kv1.2$_{419stop}$, it could distribute on the membrane surface. These observations demonstrated that the lack of ionic current for the Kv1.2$_{418stop}$ channel did not arise from its inability to traffick to the membrane surface.

4. Discussion

Our studies indicated that the HRET region in the C-terminal-truncated Kv1.2 channels could regulate the channel activation. Within the HRET region, Thr^{421} is the amino acid closest to the C-terminus. Deleting Thr^{421} (Kv1.2$_{420stop}$) or mutating it to alanine (Kv1.2$_{T421Astop}$) will make the channel more difficult to open than Kv1.2$_{421stop}$. The detailed mechanism of modulating channel activation by Thr^{421} is not clear yet. In light of the capability of Thr^{421} to be phosphorylated in the Kv1.2 channel (Munton et al., 2007), we suppose that the modulation of Thr^{421} on the channel presumably relates to its phosphorylation. Notably, the substitution of Thr at position 421 with Ser (Kv1.2$_{T421Sstop}$), which is structurally similar to Thr and can also be phosphorylated, could change the behaviour of Kv1.2$_{421stop}$. This phenomenon also

appeared in some other channels (Kuzmenkin et al., 2003; Shemon et al., 2006). It remains to be determined if the reason is due to change in phosphorylation or otherwise.

Glutamic acid, arginine and histidine are charged amino acids in the HRET region. The substitution of Glu^{420} in the C-terminal of $Kv1.2_{420stop}$ with acidic amino acid aspartic acid ($Kv1.2_{E420Dstop}$) shows a similar *G–V* curve to $Kv1.2_{420stop}$, whereas the substitution of Glu^{420} with neutral ($Kv1.2_{E420Astop}$) or basic amino acid ($Kv1.2_{E420Rstop}$) causes a distinctly leftward shift in the activation curve. As for the arginine of the C-terminal of $Kv1.2_{419stop}$, it can be substituted with basic ($Kv1.2_{R419Kstop}$) or neutral amino acid ($Kv1.2_{R419Lstop}$ and $Kv1.2_{R419Nstop}$) and displays outward currents. However, substitution of Arg^{419} with acidic amino acid ($Kv1.2_{R419Dstop}$) cannot produce a functional channel. The deletion of Arg^{419} ($Kv1.2_{418stop}$) or His^{418} ($Kv1.2_{417stop}$) produces a non-functional channel. These observations exhibited that the HRET region played a vital regulatory role for the activation of the C-terminal-truncated Kv1.2 channel.

Why is the HRET region critical for channel activation? We propose two possibilities. One possibility is that there might be a direct interaction between the HRET region and the S4-S5 linker. Although this hypothesis remains speculative, some studies have shown the directly electrostatic interactions between the Arg^{665} of the S6 end and the Asp^{540} of the S4-S5 linker in the hERG channel (Tristani-Firouzi et al., 2002; Vicente et al., 2006). Likewise, there might be direct interaction between the HRET region and the S4-S5 linker in the Kv1.2 channel. Another possibility is that mutations in the HRET region might affect the interaction between NFNYFY and the S4-S5 linker because the HRET region directly follows the NFNYFY region. These ideas are inconsistent with the Kv1.2 crystal structure, which shows that the smallest distance between some atoms of the HRET region and the S4-S5 linker or the NFNYFY region that may allow their direct interaction is less than 10 Å (Long et al., 2005b, 2005a).

We conclude that the lack of ionic current for the $Kv_{418stop}$ channel is not due to its inability to express on cell membrane because there are still some expressed $Kv1.2_{418stop}$ channels on cell membrane surface. In terms of the expression levels of the channel on cell membrane, $Kv1.2_{418stop}$ is significantly lower than $Kv1.2_{419stop}$, indicating that Arg^{419} affects the expression level of the channel on cell membrane. Besides, $Kv1.2_{418stop}$ and $Kv1.2_{419stop}$ showed lower expression levels on cell membrane surface than Kv1.2 wild type, consistent with the C-terminus containing a cluster of phosphorylation sites that regulate channel surface expression (Yang et al., 2007).

In summary, our studies suggest that the extreme C-terminus of the S6 inner helix, the HRET region, plays an important role in regulating the channel function. Further investigation will be required to clarify how these regulations take place and what their intrinsic physiological implications are.

Author contribution

Li-li Zhao carried out the experimental data collection and processing. Li-li Zhao, Zhi Qi and Xian-en Zhang participated in the design of the study. Li-li Zhao, Zhi Qi, Li-jun Bi and Gang Jin drafted the manuscript. Li-jun Bi and Gang Jin conceived and co-ordinated the study. All authors have read and approved the final manuscript.

Acknowledgements

We thank Mr Chun-Chun Liu for flow cytometry technical assistance.

Funding

This work was partly supported by the 973 programme [grant numbers 2006CB911003, 2005CB522804]; and the NSFC (National Science Foundation of China) [grant number 30470447].

References

Brew HM, Gittelman JX, Silverstein RS, Hanks TD, Demas VP, Robinson LC, et al. Seizures and reduced life span in mice lacking the potassium channel subunit Kv1.2, but hypoexcitability and enlarged Kv1 currents in auditory neurons. J Neurophysiol 2007;98:1501–25.

del Camino D, Yellen G. Tight steric closure at the intracellular activation gate of a voltage-gated K(+) channel. Neuron 2001;32:649–56.

Eunson LH, Rea R, Zuberi SM, Youroukos S, Panayiotopoulos CP, Liguori R, et al. Clinical, genetic, and expression studies of mutations in the potassium channel gene KCNA1 reveal new phenotypic variability. Ann Neurol 2000;48:647–56.

Grissmer S, Nguyen AN, Aiyar J, Hanson DC, Mather RJ, Gutman GA, Karmilowicz MJ, Auperin DD, Chandy KG. Pharmacological characterization of five cloned voltage-gated K^+ channels, types Kv1.1, 1.2, 1.3, 1.5, and 3.1, stably expressed in mammalian cell lines. Mol Pharmacol 1994;45:1227–34.

Hackos DH, Chang TH, Swartz KJ. Scanning the intracellular S6 activation gate in the shaker K+ channel. J Gen Physiol 2002;119:521–32.

Holmgren M, Smith PL, Yellen G. Trapping of organic blockers by closing of voltage-dependent K+ channels: evidence for a trap door mechanism of activation gating. J Gen Physiol 1997;109: 527–35.

Holmgren M, Shin KS, Yellen G. The activation gate of a voltage-gated K+ channel can be trapped in the open state by an intersubunit metal bridge. Neuron 1998;21:617–21.

Hopkins WF, Demas V, Tempel BL. Both N- and C-terminal regions contribute to the assembly and functional expression of homo- and heteromultimeric voltage-gated K^+ channels. J Neurosci 1994;14:1385–93.

Hoshi T, Zagotta WN, Aldrich RW. Biophysical and molecular mechanisms of Shaker potassium channel inactivation. Science 1990;250:533–8.

Jerng HH, Covarrubias M. K^+ channel inactivation mediated by the concerted action of the cytoplasmic N- and C-terminal domains. Biophys J 1997;72:163–74.

Kuzmenkin A, Jurkat-Rott K, Lehmann-Horn F, Mitrovic N. Impaired slow inactivation due to a polymorphism and substitutions of Ser-906 in the II-III loop of the human Nav1.4 channel. Pflugers Arch 2003;447:71–7.

Liu Y, Holmgren M, Jurman ME, Yellen G. Gated access to the pore of a voltage-dependent K+ channel. Neuron 1997;19:175–84.

Long SB, Campbell EB, Mackinnon R. Voltage sensor of Kv1.2: structural basis of electromechanical coupling. Science 2005a;309:903–8.

Long SB, Campbell EB, Mackinnon R. Crystal structure of a mammalian voltage-dependent Shaker family K+ channel. Science 2005b;309:897–903.
Lu Z, Klem AM, Ramu Y. Ion conduction pore is conserved among potassium channels. Nature 2001;413:809–13.
Lu Z, Klem AM, Ramu Y. Coupling between voltage sensors and activation gate in voltage-gated K+ channels. J Gen Physiol 2002;120:663–76.
Marten I, Hoshi T. The N-terminus of the K channel KAT1 controls its voltage-dependent gating by altering the membrane electric field. Biophys J 1998;74:2953–62.
Minor DL, Lin YF, Mobley BC, Avelar A, Jan YN, Jan LY, Berger JM. The polar T1 interface is linked to conformational changes that open the voltage-gated potassium channel. Cell 2000;102:657–70.
Munton RP, Tweedie-Cullen R, Livingstone-Zatchej M, Weinandy F, Waidelich M, Longo D et al. Qualitative and quantitative analyses of protein phosphorylation in naive and stimulated mouse synaptosomal preparations. Mol Cell Proteomics 2007;6:283–93.
Nesti E, Everill B, Morielli AD. Endocytosis as a mechanism for tyrosine kinase-dependent suppression of a voltage-gated potassium channel. Mol Biol Cell 2004;15:4073–88.
Rezazadeh S, Kurata HT, Claydon TW, Kehl SJ, Fedida D. An activation gating switch in Kv1.2 is localized to a threonine residue in the S2-S3 linker. Biophys J 2007;93:4173–86.
Scholle A, Dugarmaa S, Zimmer T, Leonhardt M, Koopmann R, Engeland B, Pongs O, Benndorf K. Rate-limiting reactions determining different activation kinetics of Kv1.2 and Kv2.1 channels. J Membr Biol 2004;198:103–12.
Schoppa NE, Sigworth FJ. Activation of Shaker potassium channels. II. Kinetics of the V2 mutant channel. J Gen Physiol 1998;111: 295–311.
Shemon AN, Sluyter R, Fernando SL, Clarke AL, Dao-Ung LP, Skarratt KK, et al. A Thr^{357} to Ser polymorphism in homozygous and compound heterozygous subjects causes absent or reduced P2X7 function and impairs ATP-induced mycobacterial killing by macrophages. J Biol Chem 2006;281:2079–86.
Soler-Llavina GJ, Chang TH, Swartz KJ. Functional interactions at the interface between voltage-sensing and pore domains in the Shaker K(v) channel. Neuron 2006;52:623–34.
Steidl JV, Yool AJ. Differential sensitivity of voltage-gated potassium channels Kv1.5 and Kv1.2 to acidic pH and molecular identification of pH sensor. Mol Pharmacol 1999;55:812–20.
Stuhmer W, Ruppersberg JP, Schroter KH, Sakmann B, Stocker M, Giese KP, et al. Molecular basis of functional diversity of voltage-gated potassium channels in mammalian brain. EMBO J 1989;8:3235–44.
Tristani-Firouzi M, Chen J, Sanguinetti MC. Interactions between S4-S5 linker and S6 transmembrane domain modulate gating of HERG K+ channels. J Biol Chem 2002;277:18994–19000.
Vicente R, Escalada A, Villalonga N, Texido L, Roura-Ferrer M, Martin-Satue M, et al. Association of Kv1.5 and Kv1.3 contributes to the major voltage-dependent K+ channel in macrophages. J Biol Chem 2006;281:37675–85.
Yang JW, Vacher H, Park KS, Clark E, Trimmer JS. Trafficking-dependent phosphorylation of Kv1.2 regulates voltage-gated potassium channel cell surface expression. Proc Natl Acad Sci USA 2007; 104:20055–60.
Yifrach O, MacKinnon R. Energetics of pore opening in a voltage-gated K^+ channel. Cell 2002;111:231–9.
Zhou M, Morais-Cabral JH, Mann S, MacKinnon R. Potassium channel receptor site for the inactivation gate and quaternary amine inhibitors. Nature 2001;411:657–61.

Received 26 February 2009/6 August 2009; accepted 16 September 2009

Published as Immediate Publication 16 September 2009, doi 10.1042/CBI20090009